IEEE Access
Multidisciplinary | Rapid Review | Open Access Journal

Received September 20, 2018, accepted October 11, 2018, date of publication October 22, 2018,
date of current version November 30, 2018.

Digital Object Identifier 10.1109/ACCESS.2018.2877199

Joint Resource Allocation With Weighted Max-Min Fairness for NOMA-Enabled V2X Communications

HANYU ZHENG[1], HAI LI[1], (Member, IEEE), SHUJUAN HOU[1], AND ZHENGYU SONG[2]
[1]School of Information and Electronics, Beijing Institute of Technology, Beijing 100081, China
[2]School of Electronic and Information Engineering, Beijing Jiaotong University, Beijing 100044, China

Corresponding author: Shujuan Hou (shujuanhou@bit.edu.cn)

ABSTRACT To achieve more efficient spectrum utilization in the intelligent transportation system, non-orthogonal multiple access-enabled (NOMA-enabled) V2X communications have been emerging as a promising technology. In this paper, the resource allocation problem for NOMA-enabled V2X communications is investigated. For V2I links, in view of the user fairness and the different requirements of cellular users (CUEs), weighted max-min rate fairness for CUEs is applied, where both identical weights and different weights are considered. As for V2V users (VUEs), the minimum signal-to-interference-plus-noise ratio (SINR) requirements are imposed on the problem formulation. To solve the proposed optimization problem, it is decoupled into three stages: 1) power allocation for CUEs; 2) power control and subcarrier (SC) assignment for VUE pairs; 3) SC assignment and user clustering for CUEs. For the three stages, algorithms based on the Perron-Frobenius theorem, the Kuhn-Munkres algorithm, and the matching theory are proposed separately. Finally, an algorithm integrated the three stages is presented to obtain a joint solution. The convergence and the optimality of the proposed algorithms can be verified by theoretical analysis and simulations. Moreover, simulation results also indicate that each cluster of the optimal user clustering scheme is inclined to be occupied by the CUEs with diverse channel gains and the minimum weighted rate of all CUEs, τ, will decrease with the increase of the numbers of V2V links and the minimum SINR requirements of VUE pairs.

INDEX TERMS V2X communications, non-orthogonal multiple access, resource allocation, max-min rate fairness.

I. INTRODUCTION

Vehicle to everything (V2X) communications have recently attracted significant attention, since the projected benefits can be derived from many kinds of aspects, such as decreasing traffic-related fatalities, reducing logistical costs for operating vehicular fleets and introducing a variety of new business models [1]–[4]. Attributing to the effort involving government, industry and academia, V2X communications are developing rapidly in many countries. In America, to accelerate the implementation of crash avoidance countermeasures, the Crash Avoidance Metrics Partnership (CAMP) was formed between Ford and General Motors [5]. Meanwhile, Car 2 Car Communication Consortium (C2C-CC) devotes itself to creating and establishing an open European industry standard for Cooperative Intelligent Transport Systems (C-ITS) [6].

In vehicular networks, vehicle-to-vehicle (V2V) and vehicle-to-infrastructure (V2I) are two main types of communications. Thanks to the physical proximity of communicating devices, V2V communications can provide safety-critical information imposed strict reliability and timeliness requirements [7]. With regard to V2I communications, since the high-bandwidth is available, the high-capacity and QoS-sensitive requirements of vehicles can be satisfied [8]. Meanwhile, in order to guarantee the fairness among cellular users (CUEs), some principles need to be formulated. As one of wireless access technologies to support communications in vehicular environments, LTE-based V2X (LTE-V) has been proposed for its benefits in high data rate and large coverage. To complement the insufficiency of LTE-V's centralized architecture, the technology of device-to-device (D2D) has been extended to support V2V communications [9]. Since

such communication conditions are time-varying, it is necessary to take into account rapid channel variations caused by mobility. Liang *et al.* [7] exploit the large scale fading information of the channels for resource allocation with a rigorous treatment of small-scale fading effects. Moreover, in [10], a situation of delayed channel state information (CSI) feedback is considered.

With the rising number of connected vehicles in cities, the traditional orthogonal multiple access (OMA) is inefficient due to the scarcity of spectrum band [11]. To achieve more efficient spectrum utilization, non-orthogonal multiple access (NOMA) technology has been proposed recently. Different from OMA, NOMA allows multiple users to occupy one frequency channel simultaneously, which exhibits the advantages in both spectral efficiency and cellular coverage [12]–[14]. Therefore, it can be predicted that NOMA-enabled V2X communications will be a trend in the future for its potential ability to enhance spectrum efficiency and improve user access [15].

A. RELATED WORK

Since V2I and V2V communications have absolutely different types of service requirements and may reuse the same spectrum band, it is crucial to allocate radio resource more efficiently. As a result, a great deal of research endeavor has been put into the strategies of improving the resource allocation performance. Wei *et al.* [16] study a resource allocation problem among safety V2V users (VUEs), non-safety VUEs, and conventional CUEs to maximize the system throughput. In [17], an algorithm aimed at maximizing CUEs' sum rate and guaranteeing VUEs' signal-to-interference-plus-noise ratio (SINR) requirements is proposed. To ensure the link reliability, a constraint of outage probability for VUEs is imposed on the sum rate maximization in [18]. Different from the above literature on throughput optimization, Huang *et al.* [19] apply the quality of experience (QoE) as the performance metric, which is non-linearly proportional to the data rates. In view of the saturation effect of QoE, a novel utility is formulated and a low-complexity heuristic algorithm is proposed to maximize the total utility of all devices in the V2X network. Despite these research contributing to increasing the system throughput or utility, the efforts in raising fairness among users are insufficient.

As one of the promising candidate technologies in 5G, NOMA scheme exhibits variety of advantages, such as high bandwidth efficiency, ultrahigh connectivity and compatibility [20], [21]. To make the best use of the superiority of NOMA over OMA, lots of research has been devoted to optimize the resource allocation for NOMA. In [22], a joint subcarrier (SC) and power allocation algorithm is proposed for NOMA-enabled D2D communication, which achieves promising gains in terms of network sum rate and the number of accessed users. In [23], to maximize the weighted sum rate of NOMA users, Lei *et al.* provide theoretical insights and algorithmic solutions for the problem of power and channel allocation. Since one of key features of NOMA is to balance throughput against fairness, a principle of maximizing the SINR of the worst user in each cluster is proposed in [24], which can be regarded as max-min fairness and achieve a good tradeoff between throughput and fairness.

Recently, applying NOMA scheme in V2X communications has attracted more attention due to the superiority and compatibility of NOMA [11], [25]–[28]. In [26], the long-term system-wide utility is maximized to enhance the system performance and reduce the handover rate. The optimization problem is equivalently transformed into a weighted sum rate maximization problem which can be solved by the successive convex approximation. In [27], the centralized Tx-Rx selection and resource allocation problem for vehicular devices are considered, where both time and frequency resources are needed to be fully utilized. However, in these research on NOMA-enabled V2X communications, the requirements of V2V links have not been taken into consideration, which may cause outage of the V2V communications. Also, the interference cause by VUEs may disturb the original decoding order of CUEs.

B. MOTIVATIONS AND CONTRIBUTIONS

Inspired by the aforementioned benefits of NOMA, we consider the resource allocation problem in a downlink NOMA-enabled V2X communications scenario to cope with the rapid growth number of accessed vehicles and different types of service for V2X network. Since NOMA allows multiple users to share the same SC, it has the potential to make compromise between throughput and fairness with a certain fairness principle. Hence, in this paper, the weighted max-min rate fairness is formulated in the optimization problem. Moreover, as two main types of communications, the high capacity demand of V2I links and the reliability of V2V links are of equal importance. Therefore, in our proposed resource allocation algorithms, the two kinds of requirements are guaranteed by providing a near-optimal allocation scheme for both the CUEs and VUEs. To the best of our knowledge, there has been no similar work jointly optimizing the radio resources for both CUEs and VUEs with the weighted max-min rate fairness when NOMA protocol is applied.

Our main contributions in this paper can be summarized as:

- Different from the existing work for NOMA-enable V2X communications, such as [26] and [27], we formulate the resource allocation problem with weighted max-min rate fairness for CUEs. In this paper, the data rate of each CUE is weighted according to their requirements for data service. Furthermore, the allocation algorithms for both identical weights and different weights are proposed, which achieve a good balance between throughput and fairness for CUEs.
- To guarantee the reliability of V2V links, we impose the minimum SINR requirements on the optimization problem. Moreover, we exploit all the degrees of freedom in resource allocation, including the power allocation

$\boldsymbol{p}$ and $\boldsymbol{p}^{\mathrm{v}}$, SC assignment $\boldsymbol{X}$ and $\boldsymbol{X}^{\mathrm{v}}$ for both CUEs and VUEs. Therefore, both V2I links and V2V links can reach their desired requirements. While most of the existing literature [10], [27] only deals with some of the four kinds of available resources.

- To solve the proposed optimization problem, we put forward a low complexity but efficient algorithm to decouple the optimization problem into three stages: (1) power allocation for CUEs; (2) power control and SC assignment for VUE pairs; (3) SC assignment and user clustering for CUEs. And the allocation schemes for the above subproblems are proposed separately based on Perron-Frobenius theorem, Kuhn-Munkres algorithm and matching theory. Finally, an algorithm integrated the three stages is presented to obtain a joint solution.
- The convergence and complexity of the proposed algorithm are analyzed in this paper, which can also be verified by the simulation results. Furthermore, compared to the exhaustive search method and the corresponding algorithm in OMA, it can be observed that the proposed joint resource allocation algorithm achieves near-optimal performance and applying NOMA to V2X communications shows great superiority on the spectrum utilization. Moreover, the simulation results also indicate that, in the optimal user clustering scheme, the CUEs in one cluster are probable with diverse channel gains. And the minimum weighted rate, τ, will decrease if the numbers of V2V links and the minimum SINR requirements of VUE pairs are increasing.

C. ORGANIZATION

The rest of the paper is organized as follows. In Section II, system model and problem formulation are introduced. Section III proposes the algorithms for the resource allocation in downlink NOMA-enabled V2X communications. In Section IV, we present some simulation results to illustrate the convergence and the performance of our proposed algorithms. Finally, Section V concludes this paper.

II. SYSTEM MODEL AND PROBLEM FORMULATION

A. SYSTEM MODEL

Consider a downlink NOMA-enabled V2X communication system as shown in Fig. 1, which consists of one base station (BS) with N SCs, M CUEs and K pairs of VUEs. To satisfy the high link capacity requirements of the M CUEs, they adopt power-domain NOMA scheme connecting with the BS. In a typical NOMA system, one SC is shared by multiple CUEs. Hence, we assume that $M \geq 2N$ and each CUE occupies at most one SC. Since the CUEs on each SC form a cluster, the CUE set $\mathcal{M} = \{1, 2, 3, \ldots, M\}$ is divided into N disjoint subsets and $\mathcal{M} = \mathcal{M}_1 \cup \mathcal{M}_2 \cup \ldots \cup \mathcal{M}_N$. Meanwhile, we denote $\mathcal{K} = \{1, 2, 3, \ldots, K\}$ as the K pairs of VUEs, which reuse the downlink frequency resource of CUEs. In addition, each pair of VUEs communicates with each other in the form of D2D communications. To reduce the complexity of scheduling and interference to CUEs, it is restricted that any VUE pair does not share the same SC with the other VUE pairs. Thus, we have $K \leq N$.

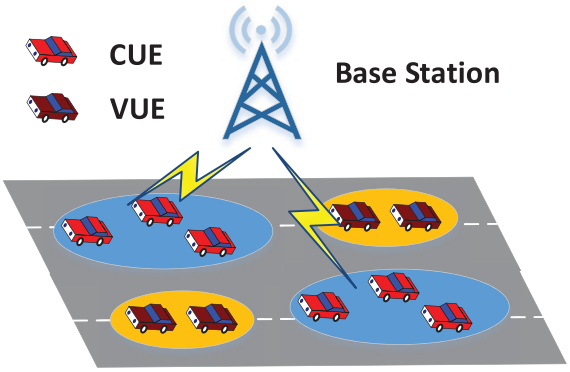

FIGURE 1. System model of downlink NOMA-enabled V2X communication.

In this paper, it is assumed that CUEs and VUEs are all equipped with a single antenna. For a downlink NOMA-enabled V2X communication system, each CUE receives messages from the BS and the VUE pair on its SC. Hence, the signal y_i received by CUE i on SC n can be expressed as

$$y_i = \sum_{i \in \mathcal{M}_n} \sqrt{p_i} H_{i,B}^n s_i + \sqrt{p_j^{\mathrm{v}}} H_{j,i}^n s_j^{\mathrm{v}} + n_0, \tag{1}$$

where p_i and s_i are the allocated power and message for CUE i, respectively. Similarly, p_j^{v} and s_j^{v} are the transmit power and message of VUE pair j. n_0 is the additive white Gaussian noise (AWGN) with variance σ^2. $H_{i,B}^n$ represents the complex channel coefficient between the BS and CUE i on SC n, and $H_{j,i}^n$ represents the complex channel coefficient between CUE i and the transmitter of VUE pair j on SC n. Furthermore, the channel gain $|H_{i,B}^n|^2$ can be expressed as

$$|H_{i,B}^n|^2 = |h_{i,B}^n|^2 \beta_{i,B} A L_{i,B}^{-\alpha}, \tag{2}$$

where $|h_{i,B}^n|^2$ denotes the small-scale fast fading power component, $\beta_{i,B}$ is a log-normal shadow fading random variable with a standard deviation ξ, A is the path loss constant, $L_{i,B}$ represents the distance from the BS to the CUE i, and α is the path loss decay exponent. As such, we define $|H_{i,j}^n|^2$ as the channel gain between CUE i and the transmitter of VUE pair j on SC n, $|G_j^n|^2$ as the channel gain between VUE pair j on SC n, and $|G_{j,B}^n|^2$ as the channel gain between the BS and the receiver of VUE pair j on SC n. In addition, we assume perfect channel state information (CSI) is available at both the transmitters and receivers. Although the practical systems are always subject to erroneous CSI, this consideration leads to a performance higher bound which serves as a benchmark for our future study in practical systems.

B. PROBLEM FORMULATION

For the resource allocation problem in a V2X system, we concern the requirements for both V2I and V2V links and allocate the resource for CUEs and VUE pairs simultaneously.

As in [7], V2I connections desire high link capacity and rate fairness among CUEs, while V2V connections place greater emphasis on link reliability. Hence, we aim to maximize the data rate of CUEs with weighted max-min rate fairness and satisfying the minimal SINR requirements of VUE pairs.

According to the downlink NOMA principle [29], a CUE with lower channel gain is allocated with more transmit power than the one with higher channel gain. Meanwhile, for CUE i, the interference caused by the signals intended for the lower channel gain CUEs on the same SC can be eliminated through the successive interference cancellation (SIC). Consequently, the lowest channel gain CUE experiences interference caused by all other CUEs in its cluster besides the VUE pair on the same SC, while the highest channel gain CUE receives interference only from the VUE pair. Due to the existence of VUE pairs, the decoding order of CUEs may be disturbed by the interference from VUE pairs. Hence, to figure out a definite decoding order of CUEs when VUE pairs exist, a normalized channel gain between the BS and CUE i is introduced as

$$\mathcal{H}_{i,B}^{n} = \frac{|H_{i,B}^{n}|^2}{\sum_{j=1}^{K} x_{j,n}^{\mathrm{v}} p_j^{\mathrm{v}} |H_{i,j}^{n}|^2 + \sigma^2}, \tag{3}$$

where $x_{j,n}^{\mathrm{v}}$ is the element of the binary matrix variable $\boldsymbol{X}^{\mathrm{v}}$ for SC assignment as

$$x_{j,n}^{\mathrm{v}} = \begin{cases} 1, & \text{if SC } n \text{ is allocated to VUE pair } j, \\ 0, & \text{otherwise.} \end{cases} \tag{4}$$

Also, the assignment matrix variable $[\boldsymbol{X}]_{i,n} = x_{i,n}$ is defined as

$$x_{i,n} = \begin{cases} 1, & \text{if SC } n \text{ is allocated to CUE } i, \\ 0, & \text{otherwise,} \end{cases} \tag{5}$$

where $[\ ]_i$ denotes the i-th element of the matrix.

Without loss of generality, the normalized channel gains of the CUEs in $\mathcal{M}_n$ are sorted in the descending order, i.e., $\mathcal{H}_{1,B}^{n} \geq \mathcal{H}_{2,B}^{n} \geq \ldots\ldots \geq \mathcal{H}_{m_n,B}^{n}$, where m_n is the number of CUEs in $\mathcal{M}_n$. Following the above decoding order, the achievable data rate $r_{i,n}$ of CUE i on SC n can be expressed as

$$r_{i,n} = \log_2 \left(1 + \frac{p_i |H_{i,B}^{n}|^2}{\sum_{k=1}^{i-1} p_k |H_{i,B}^{n}|^2 + \sum_{j=1}^{K} x_{j,n}^{\mathrm{v}} p_j^{\mathrm{v}} |H_{i,j}^{n}|^2 + \sigma^2} \right). \tag{6}$$

As a result, the total data rate of CUE i can be expressed as

$$R_i = \sum_{k=1}^{N} x_{k,n} r_{k,n}. \tag{7}$$

As for VUE pairs, the SINR γ_j^n of VUE pair j on SC n is denoted as

$$\gamma_j^n = \frac{p_j^{\mathrm{v}} |G_j^n|^2}{\sum_{i=1}^{m_n} p_i |G_{j,B}^{n}|^2 + \sigma^2}. \tag{8}$$

To satisfy the minimum SINR requirements of VUE pairs, γ_j^n should be larger than the minimum SINR threshold γ_0.

Since different CUEs could have different quality of service (QoS) requirements, the weighting parameters $\boldsymbol{w} = \{w_1, w_2, \ldots, w_M\}^T$ are imposed on each CUE. Consequently, the resource allocation problem with weighted max-min rate fairness in downlink NOMA-enabled V2X communication systems can be expressed as

$$\max_{\boldsymbol{X}, \boldsymbol{X}^{\mathrm{v}}, \boldsymbol{p}, \boldsymbol{p}^{\mathrm{v}}} \min_{i \in \mathcal{M}} \frac{R_i}{w_i} \tag{9a}$$

$$\text{s.t. } \gamma_j^n \geq \gamma_0, \quad \forall j, n, \tag{9b}$$

$$p_j^{\mathrm{v}} \leq P_{\max}, \quad \forall j, \tag{9c}$$

$$\sum_{i=1}^{M} p_i \leq P_{\text{total}}, \tag{9d}$$

$$\sum\nolimits_{n=1}^{N} x_{i,n} = 1, \quad x_{i,n} = \{0, 1\}, \ \forall i, \tag{9e}$$

$$\sum\nolimits_{i=1}^{M} x_{i,n} = m_n, \quad \forall n, \tag{9f}$$

$$\sum\nolimits_{n=1}^{N} x_{j,n}^{\mathrm{v}} = 1, \quad x_{j,n}^{\mathrm{v}} = \{0, 1\}, \quad \forall j, \tag{9g}$$

$$\sum\nolimits_{j=1}^{K} x_{j,n}^{\mathrm{v}} \leq 1, \quad \forall n, \tag{9h}$$

where $\boldsymbol{p} = \{p_1, p_2, \ldots, p_M\}^T$ and $\boldsymbol{p}^{\mathrm{v}} = \{p_1^{\mathrm{v}}, p_2^{\mathrm{v}}, \ldots, p_K^{\mathrm{v}}\}^T$ represent the power allocation schemes for CUEs and VUE pairs, respectively. Constraint (9b) is imposed to restrict the interference received by VUE pairs. Constraint (9c) indicates that each VUE pair has its maximum transmit power $P_{\max}$. Constraint (9d) guarantees that the sum of allocated power for all CUEs cannot exceed the total transmit power of the BS. In constraints (9e) and (9f), they show that each CUE occupies only one SC and SC n can be allocated to m_n CUEs. Constraints (9g) and (9h) guarantee that each VUE pair occupies one SC and each SC can be allocated to at most one VUE pair.

III. PROPOSED RESOURCE ALLOCATION ALGORITHMS

In this section, we proposed resource allocation algorithms for all the vehicular devices in the V2X system by solving optimization problem (9). For NOMA-enabled V2I links, the minimum weighted rates of CUEs are maximized based on the weighted max-min rate fairness to guarantee the high link capacity requirement and fairness of each CUE, which is regarded as the optimal control rate. Besides, the minimum SINR requirements of V2V links are imposed on the problem formulation. Hence, the proposed optimization problem is a novel formulation that NOMA protocol is adopted in V2I links and the resource allocation for both CUEs and VUEs is considered. However, the proposed optimization problem is a mixed-integer non-convex optimization problem due to the discontinuity of SC assignment variables and the complicated objective function.

To obtain a solution for optimization problem (9), we attempt to exploit the separability of optimization variables. As an operable approach, it is valid to maximize (9a)

on one or several optimization variables in successive stages when the other optimization variables are fixed. To be specific, optimization problem (9) is decomposed into three stages: (1) Power allocation for CUEs; (2) Power control and SC assignment for VUE pairs; (3) SC assignment and user clustering for CUEs. Hence, it is more tractable to derive a solution for each stage than solve (9) directly. Finally, a near-optimal solution can be obtained by the joint resource allocation algorithm which integrates the three algorithms for each stage.

A. POWER ALLOCATION FOR CUES

Suppose that Stage 2 and Stage 3 are settled, i.e., the variables $\boldsymbol{p}^{\mathrm{v}}$, $\boldsymbol{X}$ and $\boldsymbol{X}^{\mathrm{v}}$ are given. Meanwhile, the cluster set $\mathcal{M}_i$ is known. Then we define the interference ratio matrix $\boldsymbol{B}$ as

$$\boldsymbol{B} = \begin{bmatrix} \boldsymbol{B}_{1,1} & \boldsymbol{B}_{1,2} & \boldsymbol{B}_{1,3} & \dots & \boldsymbol{B}_{1,N} \\ \boldsymbol{B}_{2,1} & \boldsymbol{B}_{2,2} & \boldsymbol{B}_{2,3} & \dots & \boldsymbol{B}_{2,N} \\ \vdots & & & & \\ \boldsymbol{B}_{N,1} & \boldsymbol{B}_{N,2} & \boldsymbol{B}_{N,3} & \dots & \boldsymbol{B}_{N,N} \end{bmatrix}, \tag{10}$$

where $\boldsymbol{B}_{i,j}$ is a $m_i \times m_j$ matrix. The interference ratio matrix $\boldsymbol{B}$ is introduced to show whether or not each CUE will cause interference to other CUEs. Furthermore, if $i \neq j$, $\boldsymbol{B}_{i,j}$ is a zero matrix, which represents that the CUEs from different clusters will not cause interference to each other.

According to NOMA protocol, the CUE with lower decoding order can remove the interference caused by the CUEs with higher decoding order in one cluster. Hence, we have

$$\boldsymbol{B}_{i,i} = \begin{bmatrix} 0 & 0 & 0 & \dots & 0 & 0 \\ 1 & 0 & 0 & \dots & 0 & 0 \\ 1 & 1 & 0 & \dots & 0 & 0 \\ \vdots & & & & & \\ 1 & 1 & 1 & \dots & 1 & 0 \end{bmatrix}. \tag{11}$$

Following the above definitions, the data rate R_i can be rewritten as

$$R_i = \log_2\left(1 + \frac{p_i}{[\boldsymbol{B}\boldsymbol{p} + \boldsymbol{v}]_i}\right), \tag{12}$$

where $\boldsymbol{v} = \{v_1, v_2, \dots, v_M\}^T$ denotes the interference and noise and v_i is defined as

$$\frac{1}{|H_{i,B}^n|^2}\left(\sum_{j=1}^{K} x_{j,n}^{\mathrm{v}} p_j^{\mathrm{v}} |H_{i,j}^n|^2 + \sigma^2\right). \tag{13}$$

Since the variables $\boldsymbol{p}^{\mathrm{v}}$, $\boldsymbol{X}$ and $\boldsymbol{X}^{\mathrm{v}}$ are known in this stage, the optimization problem (9) only relates to the allocated power. Then, we define $\tau = \min\limits_{i \in \mathcal{M}} \frac{R_i}{w_i}$ as the optimal control rate. Therefore, the optimization problem (9) can be transformed as

$$\max_{\boldsymbol{p}} \ \tau \tag{14a}$$

$$\text{s.t. } \tau \boldsymbol{w} \leq \boldsymbol{R}, \tag{14b}$$

$$\gamma_0\left([\boldsymbol{G}_B\boldsymbol{p}]_j + \sigma^2\right) \leq p_j^{\mathrm{v}} |G_j^n|^2, \quad \forall j, n, \tag{14c}$$

$$\boldsymbol{D}^T\boldsymbol{p} \leq P_{\text{total}}. \tag{14d}$$

Constraint (14b) is derived from the definition of τ and $\boldsymbol{R} \triangleq \{R_1, R_2, \dots, R_M\}^T$. For the optimal τ^*, it is obvious that $\tau^*\boldsymbol{w} = \boldsymbol{R}$. In Constraint (14c), $\boldsymbol{G}_B$ is a $K \times M$ matrix, which represents the channel gains between the receivers of VUE pairs and the BS. If SC n is allocated to CUE i and VUE pair j, then $[\boldsymbol{G}_B]_{j,i} = |G_{j,B}^n|^2$. Otherwise, $[\boldsymbol{G}_B]_{j,i} = 0$. Constraint (14d) is the total power constraint and $\boldsymbol{D} = \{1, 1, \dots, 1\}^T$. It is obvious that Constraint (14c) and (14d) are transformed from Constraint (9b) and (9d). Furthermore, the other constraints in (9) are considered to be satisfied since certain values of $\boldsymbol{p}^{\mathrm{v}}$, $\boldsymbol{X}$ and $\boldsymbol{X}^{\mathrm{v}}$ are provided by Stage 2 and Stage 3.

For simplicity, Constraints (14c) and (14d) can be transformed as $\boldsymbol{Q}\boldsymbol{p} \leq \boldsymbol{q}$, where $\boldsymbol{Q} = [\boldsymbol{G}_B; \boldsymbol{D}^T]$. As for the first K elements of $\boldsymbol{q}$, we have $q_j = p_j^{\mathrm{v}}|G_j^n|^2/\gamma_0 - \sigma^2$ and the last element of $\boldsymbol{q}$ equals to P_{total}. Hence, we denote $\mathcal{K}'$ as the set of the $K+1$ constraints, which can be expressed as

$$(1/q_j)\boldsymbol{e}_j^T\boldsymbol{Q}\boldsymbol{p} \leq 1, \quad \forall j \in \mathcal{K}', \tag{15}$$

where $\boldsymbol{e}_j$ is the standard orthogonal basis.

Meanwhile, according to (12), we have

$$2^{R_i} = \frac{p_i}{[\boldsymbol{B}\boldsymbol{p} + \boldsymbol{v}]_i} + 1, \tag{16}$$

which can be expressed in matrix form as

$$\left(\text{diag}(2^{\boldsymbol{R}}) - \boldsymbol{I}\right)(\boldsymbol{B}\boldsymbol{p} + \boldsymbol{v}) = \boldsymbol{p}. \tag{17}$$

Substituting (15) into (17), Constraints (14c) and (14d) can be further rewritten as

$$\left(\text{diag}(2^{\boldsymbol{R}}) - \boldsymbol{I}\right)\left(\boldsymbol{B} + (1/q_j)\boldsymbol{v}\boldsymbol{e}_j^T\boldsymbol{Q}\right)\boldsymbol{p} \leq \boldsymbol{p}, \quad \forall j \in \mathcal{K}'. \tag{18}$$

which can be transformed based on Perron-Frobenius theorem [30] as

$$\rho\left((\text{diag}(2^{\boldsymbol{R}}) - \boldsymbol{I})(\boldsymbol{B} + (1/q_j)\boldsymbol{v}\boldsymbol{e}_j^T\boldsymbol{Q})\right) \leq 1, \quad \forall j \in \mathcal{K}', \tag{19}$$

where $\rho(\boldsymbol{M})$ denotes the spectral radius of matrix $\boldsymbol{M}$. Note that $v_i > 0$ and each line of $\boldsymbol{Q}$ contains at least m_n positive elements. Hence, in the diagonal direction of matrix $(\boldsymbol{B} + (1/q_j)\boldsymbol{v}\boldsymbol{e}_j^T\boldsymbol{Q})$, there exists a $m_n \times m_n$ positive submatrix at least, which satisfies Perron-Frobenius theorem. As a result, $\boldsymbol{p}$ is a strictly positive eigenvector associated with ρ.

Since (19) is monotone increasing and $\tau\boldsymbol{w} \leq \boldsymbol{R}$ as in (14b), the optimization problem (14) can be equivalently rewritten as

$$\max_{\boldsymbol{p}} \ \tau \tag{20a}$$

$$\text{s.t. } \rho\left((\text{diag}(2^{\tau\boldsymbol{w}}) - \boldsymbol{I})(\boldsymbol{B} + (1/q_j)\boldsymbol{v}\boldsymbol{e}_j^T\boldsymbol{Q})\right) \leq 1, \quad \forall j \in \mathcal{K}'. \tag{20b}$$

Note that if $\boldsymbol{w}$ is identical for all CUEs, optimization problem (20) can be further simplified. Hence, we propose the power allocation algorithm considering both the following two cases.

Case 1: Identical weights for CUEs.

For identical weights, Constraint (20b) can be converted as

$$(2^{\tau}-1)\rho\left(\boldsymbol{B}+(1/q_j)\boldsymbol{v}\boldsymbol{e}_j^T\boldsymbol{Q}\right)\leq 1,\quad j\in\mathcal{K}'. \tag{21}$$

Therefore, the optimal τ^* can be derived as

$$\tau^*=\log_2(1/\rho_{\max}+1), \tag{22}$$

where $\rho_{\max}=\max_{j\in\mathcal{K}'}\{\rho\left(\boldsymbol{B}+(1/q_j)\boldsymbol{v}\boldsymbol{e}_j^T\boldsymbol{Q}\right)\}$.

Case 2: Different weights for CUEs.

Since the spectral radius ρ is monotonically increasing of τ, maximizing τ in (20b) leads to at least one of the constraints in $\mathcal{K}'$ becoming tight at optimality. Due to the complexity of calculating τ^* directly, an algorithm based on binary search is proposed. Before searching, a search interval of τ needs to be specific. Since $\tau=\min_{i\in\mathcal{M}}\frac{R_i}{w_i}$, it is obvious that

$$\tau\leq\frac{\sum_{i=1}^{M}R_i}{\sum_{i=1}^{M}w_i}. \tag{23}$$

Furthermore, the numerator of the right side in (23) can be regarded as the system throughput of CUEs. To find an upper bound of the system throughput, we assume that CUE l who has the largest channel gain among all CUEs is allocated with the total transmit power. Apparently, due to the interference among CUEs and VUE pairs, we have

$$\sum_{i=1}^{M}R_i<\log_2\left(1+\frac{P_{\text{total}}|H_{l,B}^n|^2}{\sigma^2}\right). \tag{24}$$

Consequently, the upper bound of the search interval τ^{up} can be defined as

$$\tau^{\text{up}}=\log_2\left(1+\frac{P_{\text{total}}|H_{l,B}^n|^2}{\sigma^2}\right)\Big/\sum_{i=1}^{M}w_i \tag{25}$$

Since $\tau^*>0$, we define $\tau^{\text{down}}=0$ and the search interval is limited in $(\tau^{\text{down}},\tau^{\text{up}})$. Meanwhile, to simplify the expression, $f(\tau)$ is defined as

$$f(\tau)=\max_{j\in\mathcal{K}'}\{\rho((\text{diag}(2^{\tau\boldsymbol{w}})-\boldsymbol{I})(\boldsymbol{B}+\frac{1}{q_j}\boldsymbol{v}\boldsymbol{e}_j^T\boldsymbol{Q}))\}. \tag{26}$$

As displayed in **Algorithm 1**, the power allocation for CUEs (PAC) algorithm is provided and the search procedures are listed in Case 2. In addition, after obtaining τ^*, the optimal power allocation vector $\boldsymbol{p}^*$ can be derived with the following theorem.

Theorem 1: For the optimal τ^*, $\boldsymbol{p}^*$ is given by

$$\boldsymbol{p}^*=\left(\boldsymbol{I}-(\text{diag}(2^{\tau^*\boldsymbol{w}})-\boldsymbol{I})\boldsymbol{B}\right)^{-1}\left(\text{diag}(2^{\tau^*\boldsymbol{w}})-\boldsymbol{I}\right)\boldsymbol{v}, \tag{27}$$

Proof: As in (17), we have

$$\left(\boldsymbol{I}-(\text{diag}(2^{\tau\boldsymbol{w}})-\boldsymbol{I})\boldsymbol{B}\right)\boldsymbol{p}=(\text{diag}(2^{\tau\boldsymbol{w}})-\boldsymbol{I})\boldsymbol{v}. \tag{28}$$

Due to the increasing monotonicity of the spectral radius function, it can be derived that $\rho\left((\text{diag}(2^{\tau\boldsymbol{w}})-\boldsymbol{I})\boldsymbol{B}\right)<\rho\left((\text{diag}(2^{\tau\boldsymbol{w}})-\boldsymbol{I})(\boldsymbol{B}+(1/q_j)\boldsymbol{v}\boldsymbol{e}_j^T\boldsymbol{Q})\right)\leq 1$, which indicates that $\left(\boldsymbol{I}-(\text{diag}(2^{\tau^*\boldsymbol{w}})-\boldsymbol{I})\boldsymbol{B}\right)$ is an invertible matrix. Thus, (27) can be obtained. ■

Algorithm 1 PAC Algorithm

Input: feasible schemes of $\boldsymbol{p}^{\text{v}}$, $\boldsymbol{X}$ and $\boldsymbol{X}^{\text{v}}$.

For Case 1:

1) Calculate the maximum spectral radius $\rho_{\max}$ of the $K+1$ constraints as
$$\rho_{\max}=\max_{j\in\mathcal{K}'}\{\rho\left(\boldsymbol{B}+(1/q_j)\boldsymbol{v}\boldsymbol{e}_j^T\boldsymbol{Q}\right)\}.$$
2) The optimal τ^* can be derived as
$$\tau^*=\log_2(1/\rho_{\max}+1).$$

For Case 2:

Initialization: Set $k=0$ and $(\tau^{\text{down}},\tau^{\text{up}})$ denotes the search interval.

repeat

1) $\tau(k)=(\tau^{\text{down}}+\tau^{\text{up}})/2$.

if $f(\tau(k))<1$ **then**

2) $\tau^{\text{down}}=\tau(k)$;

else

3) $\tau^{\text{up}}=\tau(k)$;

end if

4) Set $k=k+1$.

until $f(\tau(k))=1$ **or** $|\tau^{\text{up}}-\tau^{\text{down}}|<\epsilon$.

Thus, $\boldsymbol{\tau(k)}\rightarrow\boldsymbol{\tau^*}$.

Output: As in (27), the optimal power allocation vector $\boldsymbol{p}^*$ can be derived with τ^*.

Given the proposed PAC algorithm above, the remarks on the optimality, convergence and complexity are presented as follows:

1) Optimality: To ensure the optimality, the following conditions need to hold for $j=1,2,\ldots K$

$$q_j=p_j^{\text{v}}|G_j^n|^2/\gamma_0-\sigma^2>0 \tag{29}$$

Hence, we have $\gamma_0<p_j^{\text{v}}|G_j^n|^2/\sigma^2$. Note that the constraints in (20) are transformed from constraints in (14) which are composed of linear power inequalities. Thus, it is obvious that the feasible set for τ must be not a null set.

To further verify the uniqueness of τ^*, we notice that τ^* can be uniquely determined through PAC algorithm in Case 1. While in Case 2, τ can not be maximized any more if one of constraints become tight, since the spectral radius function is monotonically increasing of τ [30]. Consequently, with a given search interval, the optimal τ^* can be always obtained.

2) Convergence:

Lemma 1: The number of iterations required by PAC algorithm in Case 2 is upper bounded by $\lceil\log_2\left(|\tau^{\text{up}}-\tau^{\text{down}}|/\epsilon\right)\rceil$.

Proof: The proposed PAC algorithm can always converge to the optimal τ^* within a deviation ϵ in Case 2. Since $\tau^{\text{up}}>\tau^*$ and $\tau^{\text{down}}<\tau^*$, it can be concluded that $f(\tau^*)=1$ is located in the search interval due to the increasing monotonicity of $f(\tau)$. Meanwhile, as in PAC algorithm, the length of the search interval declines to half in each iteration. Hence,

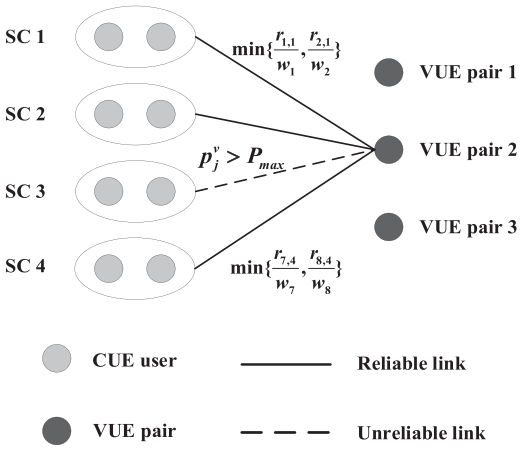

FIGURE 2. An example of the matching between SCs and VUE pairs.

in the m-th iteration, the length of the search interval equals to $(\tau^{\text{up}} - \tau^{\text{down}})/2^m$. Furthermore, for the worst case, PAC algorithm will stop searching if $(\tau^{\text{up}} - \tau^{\text{down}})/2^m$ is less than ϵ, which means that the total number of iterations is upper bounded by $\lceil \log_2 \left(|\tau^{\text{up}} - \tau^{\text{down}}|/\epsilon \right) \rceil$. ■

3) Complexity: For each iteration in PAC algorithm, the computational complexity is mainly affected by the calculation of $f(\tau(k))$ which is the largest one of $K+1$ spectral radii. Since the computational complexity of each spectral radius is related to the number of elements in matrix $(\text{diag}(2^{\tau(k)}\boldsymbol{w}) - \boldsymbol{I})(\boldsymbol{B} + \frac{1}{q_j}\boldsymbol{v}\boldsymbol{e}_j^T\boldsymbol{Q})$, the computational complexity of computing each spectral radius is $\mathcal{O}(M^2)$. As a result, the total computational complexity of PAC algorthm is $\mathcal{O}(KM^2)$.

B. POWER CONTROL AND SC ASSIGNMENT FOR VUE PAIRS

In this part, the problem of power control and SC assignment for VUE pairs is considered. Assume the resource allocation for CUEs has been settled. Thus, in optimization problem (9), $\boldsymbol{p}^{\text{v}}$ and $\boldsymbol{X}^{\text{v}}$ are the only optimization variables to be solved, which can be reformulated as

$$\max_{\boldsymbol{p}^{\text{v}},\boldsymbol{X}^{\text{v}}} \min_{i\in\mathcal{M}} \frac{r_{i,n}}{w_i} \tag{30a}$$

$$\text{s.t. } \gamma_j^n \geq \gamma_0, \quad \forall j, n, \tag{30b}$$

$$p_j^{\text{v}} \leq P_{\max}, \quad \forall j, \tag{30c}$$

$$\sum_{n=1}^{N} x_{j,n}^{\text{v}} = 1, \quad x_{j,n}^{\text{v}} = \{0,1\}, \ \forall j, \tag{30d}$$

$$\sum_{j=1}^{K} x_{j,n}^{\text{v}} \leq 1, \quad \forall n. \tag{30e}$$

The optimization problem in (30) can be modeled as a problem of bipartite graph matching. To solve problem (30) efficiently, the power control and SC assignment for VUE pairs (PCSAV) algorithm is proposed based on maximum weight matching (MWM).

In Fig. 2, an example of the matching between SCs and VUE pairs is illustrated. The vertex set of the bipartite graph in Fig. 2 is partitioned into two subsets as SC set and VUE pair set. Thus, the problem of power control and SC assignment for VUE pairs can be solved by searching a MWM between SCs and VUE pairs. To maximize $\min_{i\in\mathcal{M}} \frac{r_{i,n}}{w_i}$, it is helpful to decrease p_j^{v} as far as possible in order to reduce the interference to CUEs. Therefore, for each edge, the minimum p_j^{v} makes Constraint (30b) tight, which is given by

$$p_j^{\text{v}} = \frac{\gamma_0 \left(\sum_{i=1}^{m_n} p_i |G_{j,B}^n|^2 + \sigma^2 \right)}{|G_j^n|^2}. \tag{31}$$

The solid edges in Fig. 2 represent reliable link for VUE pairs, which means that p_j^{v} in (31) is less than $P_{\max}$. And the dashed edges denote unreliable link for VUE pairs. For example, SC 3 cannot be allocated to VUE pair 2 due to $p_j^{\text{v}} > P_{\max}$. Thus, only the SCs connected to solid edges can be allocated to the corresponding VUE pairs. Furthermore, each solid edge is weighted by $\min_{i\in\mathcal{M}_n} \frac{r_{i,n}}{w_i}$ as in Fig. 2. To obtain a matching with maximum $\min_{i\in\mathcal{M}} \frac{r_{i,n}}{w_i}$, the SC assignment algorithm based on Kuhn-Munkres algorithm [31] is proposed and the whole PCSAV algorithm is presented in **Algorithm 2**. The computational complexity of the first two steps is given by $\mathcal{O}(KN)$. As for the step 3), a complexity of $\mathcal{O}(NK^2)$ is required.

Algorithm 2 PCSAV Algorithm

Input: power allocation and user clustering results of CUE, $\boldsymbol{p}$ and $\boldsymbol{X}$.
for $n = 1 : N$ **do**
  for $j = 1 : K$ **do**
    1) For each pair of (SC n, VUE pair j), check the reliability of the link by calculating p_j^{v} via (31).
    if $p_j^{\text{v}} < P_{\max}$ **then**
      2) Derive the weight $\min_{i\in\mathcal{M}_n} \frac{r_{i,n}}{w_i}$ of each reliable link.
    end if
  end for
end for
3) Apply Kuhn-Munkres algorithm to obtain $\boldsymbol{X}^{\text{v}}$ and the p_j^{v} in MWM constructs the optimal $\boldsymbol{p}^{\text{v}}$.
Output: the optimal power $\boldsymbol{p}^{\text{v}}$ and SC assignment $\boldsymbol{X}^{\text{v}}$ for VUE pairs.

C. SC ASSIGNMENT AND USER CLUSTERING FOR CUES

In this stage, we are concerned about the problem of SC assignment and user clustering for CUEs. Supposing $\boldsymbol{p}^{\text{v}}$ and $\boldsymbol{X}^{\text{v}}$ are fixed, then the optimization problem (9) can be transformed as

$$\max_{\boldsymbol{p},\boldsymbol{X}} \min_{i\in\mathcal{M}} \frac{R_i}{w_i} \tag{32a}$$

$$\text{s.t. } \sum_{i=1}^{M} p_i \leq P_{\text{total}}, \tag{32b}$$

$$\sum_{n=1}^{N} x_{i,n} = 1, x_{i,n} = \{0,1\}, \quad \forall i, \tag{32c}$$

$$\sum_{i=1}^{M} x_{i,n} = m_n, \quad \forall n, \tag{32d}$$

which is a mixed-integer non-convex optimization problem. Since it requires exponential computational complexity to obtain its optimum for exhaustive search method, a low-complexity and effective algorithm based on matching theory [32], [33] is proposed in this paper.

The M CUEs and N SCs from two disjoint sets act as rational players to maximize their own benefits, which can be mapped as a problem of bipartite matching. Different from SC assignment for VUE pairs which is a one to one matching, in this stage, multiple CUEs can share the same SC simultaneously. To introduce the CUE-SC matching algorithm, the following definitions are first given.

Definition 1 (A Many-to-One Two-Sided Matching Problem With External Effect): Since NOMA protocol is applied for CUEs and each CUE is assumed to occupy one SC, a *many-to-one* matching algorithm is required to solve optimization problem (32). Furthermore, in the scenario of CUE-SC matching, it is a *two-sided* matching problem, which means that not only CUEs have chance to choose a favourite SC but also SCs may prefer a group of CUEs to others. Meanwhile, note that the decision of each SC to match with one CUE can be affected by the actions of other CUEs, which implies that this matching problem has *external effect*.

Definition 2 (Preference): A blocking pair is denoted by $(\mathrm{CUE}_i, \mathrm{SC}_n)$, which represents the assignment that SC n is allocated to CUE i. In this CUE-SC matching problem, both CUEs and SCs choose their partners according to their own *preferences*. In addition, $V_i^{\mathrm{CUE}}(\mathrm{CUE}_i, \mathrm{SC}_n)$ and $V_n^{\mathrm{SC}}(\mathrm{CUE}_i, \mathrm{SC}_n)$ are defined as the matching values of CUE i and SC n, respectively. Hence, for CUE i, the preference can be expressed by an order of matching value as:

$$V_i^{\mathrm{CUE}}(\mathrm{CUE}_i, \mathrm{SC}_n) \succeq V_i^{\mathrm{CUE}}(\mathrm{CUE}_i, \mathrm{SC}_m) \Leftrightarrow r_{i,n} \geq r_{i,m}, \tag{33}$$

which implies that CUE i prefers SC n to SC m. Similarly, for SC n, we have

$$V_n^{\mathrm{SC}}(\mathrm{CUE}_i, \mathrm{SC}_n) \succeq V_n^{\mathrm{SC}}(\mathrm{CUE}_j, \mathrm{SC}_n) \Leftrightarrow \min_{k\in\{\mathcal{M}_n\cup i\}} \frac{R_k}{w_k} \geq \min_{k\in\{\mathcal{M}_n\cup j\}} \frac{R_k}{w_k}. \tag{34}$$

Definition 3 (Swap Rule): For a given matching Γ, it is assumed that $\mathrm{CUE}_i \in \mathcal{M}_n$ and $\mathrm{CUE}_j \in \mathcal{M}_m$. Consider a new matching Γ' with $\mathcal{M}_n' = \{\mathcal{M}_n \setminus i \cup j\}$ and $\mathcal{M}_m' = \{\mathcal{M}_m \setminus j \cup i\}$. Furthermore, CUE i may execute a swap with CUE j if the following conditions are satisfied:

$$r_{i,n} > r_{i,m'} \tag{35a}$$

$$\min_{k\in\{\mathcal{M}_n'\cup\mathcal{M}_m'\}} \frac{R_k}{w_k} \geq \min_{k\in\{\mathcal{M}_n\cup\mathcal{M}_m\}} \frac{R_k}{w_k}, \tag{35b}$$

which indicates that both CUE i and SC n prefers Γ' to Γ.

Following the above definitions, the proposed SC assignment and user clustering for CUEs (SAUCC) algorithm can converge to the sub-optimal solution by keeping searching an executable swap. As highlighted in **Algorithm 3**, SAUCC algorithm contains two phases named as initial phase and swap phase. In the initial phase, a heuristic allocation scheme Γ_0 is proposed. While in the swap phase, the matching Γ is updated according to the swap rule. As for the convergence and computation complexity, they will be verified in Section III.D.

Algorithm 3 SAUCC Algorithm

Input: the optimal power $\boldsymbol{p}^{\mathrm{v}}$ and SC assignment $\boldsymbol{X}^{\mathrm{v}}$ for VUE pairs.
Initial Phase:
Set $\mathcal{M}_n = \varnothing$, $1 \leq n \leq N$ and $\mathcal{U} = \mathcal{M}$. s_n is denoted as the number of CUEs in $\mathcal{M}_n$ whose initial value is zero.
repeat
  for $n = 1 : N$ **do**
    if $s_n < m_n$ **then**
      1) $t = \arg\max_{i\in\{\mathcal{M}_n\cup i\}} \min \frac{R_i}{w_i}$, $i \in \mathcal{U}$.
      2) $\mathcal{M}_n = \{\mathcal{M}_n \cup t\}$, $s_n = s_n + 1$.
      3) $\mathcal{U} = \{\mathcal{U} \setminus t\}$.
    end if
  end for
until $\mathcal{U} = \varnothing$.
Denote the current matching as Γ_0.
Swap Phase:
For a given Γ_0:
repeat
  for $i = 1 : M$, suppose $i \in \mathcal{M}_n$ **do**
    for $j = 1 : M$, and $j \notin \mathcal{M}_n$ **do**
      4) Swap CUE i with CUE j if (35) is satisfied, and denote this matching as $\Gamma(i, j)$.
      5) Apply PAC algorithm for $\Gamma(i, j)$ and record $\tau(i, j)$ as the optimal rate control result of $\Gamma(i, j)$.
      6) CUE i and CUE j go back to their original SCs.
    end for
    7) Perform the swap with the maximum $\tau(i, j)$.
  end for
until no CUEs are willing to change their matchings.
The final matching Γ_{final} is obtained. Meanwhile, the power allocation scheme of Γ_{final} has been solved in step 5) with PAC algorithm.
Output: power allocation and user clustering results of CUE, $\boldsymbol{p}$ and $\boldsymbol{X}$.

D. ALGORITHM FOR THE JOINT OPTIMIZATION PROBLEM

With the above three algorithms, we proposed the following resource allocation algorithm to solve optimization problem (9) jointly. Since the four optimization variables are interdependent, it always requires to fix several variables and derive the others. Hence, in our proposed NOMA-enabled V2X system resource allocation (NVRA) algorithm, initial values of optimization variables should be given first.

To run NVRA algorithm, we propose a heuristic method as initialization, which provides the initial values of $\boldsymbol{p}^{\mathrm{v}}$ and

Algorithm 4 NVRA Algorithm

Input: Set $k = 0$, $p_j^{\mathrm{v}} = P_{\max}$ and each edge connecting VUE pair and SC is weighted by $\frac{|G_j^n|^2}{|G_{j,B}^n|^2}$.

1) Apply Kuhn-Munkres algorithm to obtain an initial $\boldsymbol{X}^{\mathrm{v}}$.
2) The Initial Phase of SAUCC algorithm is conducted to derive an initial matching Γ_0.

repeat

3) The Swap Phase of SAUCC algorithm is applied with PAC algorithm to solve the problem of resource allocation for CUEs. Denote the optimal control rate as $\tau_s(k)$.
4) Update power control and SC assignment scheme for VUE pairs with PCSAV algorithm. And the optimal control rate is increased from $\tau_s(k)$ to $\tau_p(k)$.
5) Set $k = k + 1$.

until $0 < \tau_p(k) - \tau_p(k-1) < \epsilon$.

Output: Both the power allocation and SC assignment schemes for CUEs and VUE pairs.

$\boldsymbol{X}^{\mathrm{v}}$. For instance, p_j^{v} is set to be $P_{\max}$ at beginning and then optimized in the following stages. Meanwhile, in order to reduce the transmit power of VUE pairs, it is reasonable for VUE pair to choose a SC with higher channel gain and lower interference. As a result, a SC assignment based on MWM is proposed, where the weight equals to $|G_j^n|^2/|G_{j,B}^n|^2$. Then, PAC algorithm, SAUCC algorithm and PCSAV algorithm are applied in succession as displayed in **Algorithm 4**.

We next analyze the convergence and computation complexity of NVRA algorithm as following:

1) Convergence:

Lemma 2: For a given deviation of ϵ, NVRA algorithm converges within limited numbers of swaps.

Proof: Since the total power P_{total} of the BS and the number of SCs are finite, it is obvious that the optimal control rate (9a) has an upper bound. For a given $\boldsymbol{X}^{\mathrm{v}}$ and $\boldsymbol{p}^{\mathrm{v}}$, SAUCC algorithm in step 3) can always converge to Γ_{final} due to its increasing monotonicity. Mathematically, the matching transformations can be expressed as

$$\Gamma_0 \to \Gamma_1 \to \Gamma_2 \to \cdots \to \Gamma_{\mathrm{final}-1} \to \Gamma_{\mathrm{final}}. \tag{36}$$

Since the optimal control rate $\tau_s(k)$ is upper bounded and increased after each swap, SAUCC algorithm must converge to Γ_{final} within limited numbers of swaps. To further increase the optimal control rate $\tau_s(k)$, PCSAV algorithm is applied in step 4) by adjusting the results of $\boldsymbol{X}^{\mathrm{v}}$ and $\boldsymbol{p}^{\mathrm{v}}$ with fixed $\boldsymbol{X}$ and $\boldsymbol{p}$. Hence, the optimal control rate is increased from $\tau_s(k)$ to $\tau_p(k)$. Then a new iteration of SAUCC algorithm with limited numbers of swaps is started. Overall, the optimal control rate τ is monotonically increasing and upper bounded, which guarantees that the total number of swaps is limited for a given deviation of ϵ. ■

2) Complexity: As in NVRA algorithm, the computation complexity is mainly determined by step 3) and step 4). With regard to SAUCC algorithm, at most M^2 potential swap pairs need to be considered in each iteration. In addition, PAC algorithm called in step 5) of SAUCC algorithm requires a computation complexity as $\mathcal{O}(KM^2)$. Consequently, the total computation complexity of SAUCC algorithm is $\mathcal{O}(KM^4)$.

As for step 4) of NVRA algorithm, a complexity of $\mathcal{O}(NK^2)$ is required, which leads to polynomial computational complexity as $\mathcal{O}(KM^4 + NK^2)$ for the whole NVRA algorithm.

TABLE 1. Simulation parameters.

Parameter	Value
Carrier frequency	2GHz
Bandwidth	10MHz
Lane width	50m
BS total transmit power	40dBm
BS antenna gain	8dBi
VUE pair maximum transmit power	15dBm
VUE antenna gain	3dBi
minimum SINR requirements of VUE pairs	5dB,8dB,11dB
Path loss for CUEs	128.1+37.6log(d[km])
Path loss for VUE pairs	148.1+40log(d[km])
Standard deviation of shadow fading (V2I)	8dB
Standard deviation of shadow fading (V2V)	3dB
Fast fading	Rayleigh model
Noise power	-174dBm/Hz
Noise figure	9dB

IV. NUMERICAL RESULTS

In this section, simulation results are provided to illustrate the performance of the proposed NVRA algorithm for the joint resource allocation in downlink NOMA-enabled V2X communication systems. Some simulation parameters are listed in Table 1. In addition, to reduce the decoding complexity and restrict the error propagation when performing SIC, it is helpful to keep the number of CUEs on each SC approximately equal, i.e., $m_n = M/N$.

A. CONVERGENCE AND OPTIMALITY

Power allocation for CUEs by using PAC algorithm is one of the main tasks in the proposed NVRA algorithm. For Case 1, the optimal τ^* can be derived directly. With regard to Case 2, PAC algorithm based on binary search is proposed to obtain the optimal τ^* within a deviation ϵ. To verify the convergence of PAC algorithm for Case 2, a specific simulation scenario is considered. We set $N = 4, M = 12, K = 2$ and the weights of CUEs are randomly generated. As shown in Fig. 3(a), the spectral radius function is monotonically increasing with τ. Meanwhile, following Constraint (20b), the solution of $\rho = 1$ is searched via PAC algorithm to obtain the optimal τ^*. According to (25), the initial search interval is given by $(0, 22.4531)$. Furthermore, we set $\epsilon = 10^{-5}$. Hence, the maximum number of the iterations can be calculated from $\lceil \log_2 \left(|\tau^{\mathrm{up}} - \tau^{\mathrm{down}}|/\epsilon \right) \rceil$, which is almost twenty times for the above situation. As displayed in Fig. 3(b), after near 8 iterations, the search result is quite close to the optimal τ^*.

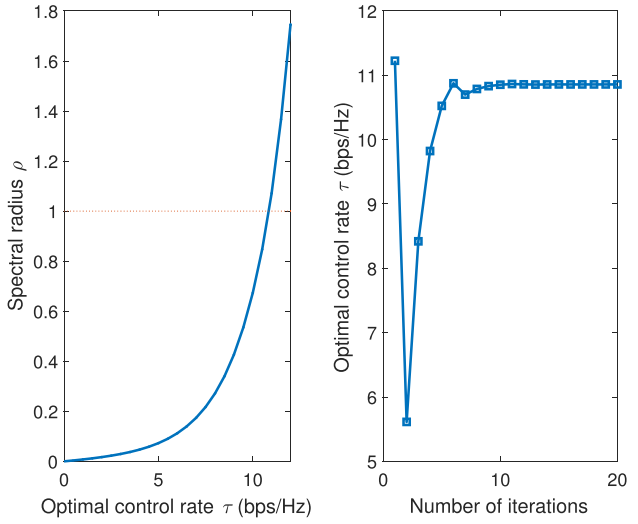

(a) (b)

FIGURE 3. (a) Spectral radius ρ versus optimal control rate τ. (b) The total iterations of binary search in PAC algorithm.

SAUCC algorithm is aimed to solve SC assignment and user clustering for CUEs, which is based on matching theory. The optimal τ^* is increased after each swap until no swap pair can be formed. To figure out the number of swaps required in general, the cumulative distribution function (C.D.F) of the number of swaps is obtained followed by Monte Carlo method. Hence, the convergence of SAUCC algorithm and NVRA algorithm is evaluated in Fig. 4. Since the simulation results in Case 1 or Case 2 have no impact on the number of swaps, in this scenario, identical weights for CUEs are adopted. In Fig. 4(a), it shows the C.D.F. of the number of swaps y_s in SAUCC algorithm. It can be observed that on average a maximum of 60 iterations are needed to converge for $M = 30, N = 5$, which verifies the convergence of SAUCC algorithm. Furthermore, since the increase of M or N means more potential user clustering options, SAUCC algorithm needs larger number of swaps to converge to the final state, where the growth of N has a relatively less impact on y_s.

In Fig. 4(b), the C.D.F. of the total number of swaps y_{total} in NVRA algorithm is presented. Note that in each iteration of NVRA algorithm, new swaps may be formed if the allocation results of VUE pairs are changed. Hence, we set that the number of VUE pairs K equals to the number of SCs N, which may need more swaps to converge. As expected, NVRA algorithm requires more swaps than SAUCC algorithm, though the two C.D.F.s have a similar trend. Also, as marked in Fig. 4, the difference of y_{total} and y_s is less than y_s in general, which means that the number of swaps required in each iteration in NVRA algorithm is gradually reduced. Therefore, the convergence of NVRA algorithm is confirmed.

To evaluate the performance of the proposed NVRA algorithm, the following three schemes are conducted to serve as benchmarks:

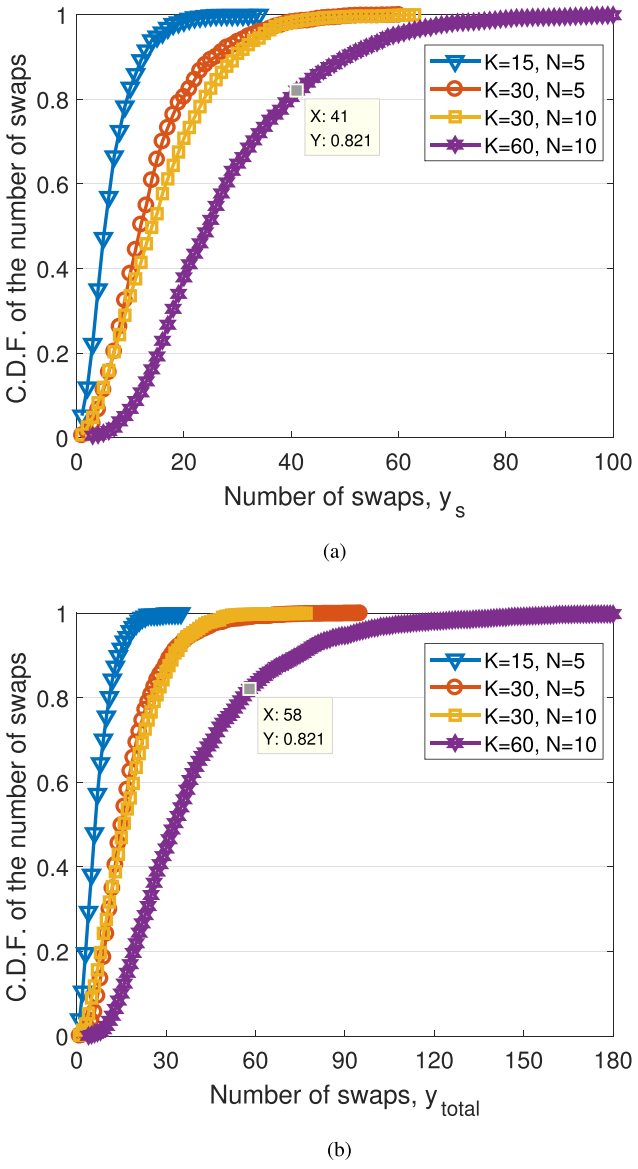

FIGURE 4. Distributions of the total number of swaps in SAUCC algorithm and NVRA algorithm ($K = N$). (a) C.D.F. of the number of swaps in SAUCC algorithm. (b) C.D.F. of the number of swaps in NVRA algorithm.

- **Exhaustive search:** In step 2) of NVRA algorithm, SAUCC algorithm based on matching theory is applied to search an approximate optimal result. In order to provide an optimal result for SC assignment and user clustering, exhaustive search method is adopted in step 2) of NVRA algorithm to serve as a benchmark.
- **Max-Min Rate Proportional Fairness:** This scheme aimed at maximizing $\min_{i\in\mathcal{M}_n} \frac{r_{i,n}(t)}{T_{i,n}(t)}$ is proposed in [34], where t denotes a period of duration and $T_{i,n}(t)$ represents the accumulative data rate of CUE i in the past time.
- **OMA-enabled V2X:** For OMA-enabled V2X, all CUEs choose TDMA mode to communicate with the BS. To achieve max-min rate fairness, the transmit power and transmit interval for each CUE are optimized.

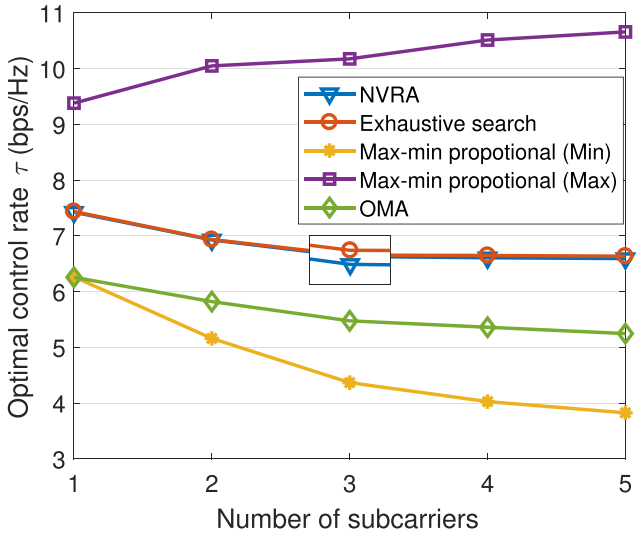

FIGURE 5. The optimal control rate τ versus the number of SCs with different schemes. ($M = 2N, K = N, \gamma_0 = 8$dB).

TABLE 2. SC assignment and user clustering schemes.

	$\gamma_0 = 5$dB	$\gamma_0 = 8$dB	$\gamma_0 = 11$dB
SC 1	C_3, C_6, C_9	C_3, C_9, C_{12}	C_7, C_9, C_{11}
SC 2	C_2, C_7, C_{10}, V_1	C_4, C_7, C_{10}, V_1	C_1, C_3, C_{10}, V_1
SC 3	C_1, C_8, C_{11}, V_3	C_5, C_8, C_{11}, V_2	C_4, C_8, C_{12}, V_2
SC 4	C_4, C_5, C_{12}, V_2	C_1, C_2, C_6, V_3	C_2, C_5, C_6, V_3
τ^*	7.05741	6.89361	6.07282

In Fig. 5, the optimal control rates of the above three schemes are provided for comparisons, where the number of CUEs in one cluster is assumed to be two and the number of VUE pairs is supposed to be N. It can be seen that NVRA algorithm achieves near-optimal τ compared to the exhaustive search method which requires exponential complexity. According to [34], the data rates of the farthest user and the nearest user are also displayed, which are denoted by "Min" and "Max", respectively. As shown in Fig. 5, the τ of NVRA algorithm is between the data rates of the farthest user and the nearest user in [34]. Mathematically, the optimization formulation of [34] is similar to the weighted max-min rate fairness in this paper. Nevertheless, the difference is that the weights considered in NVRA algorithm can be adjusted flexibly according to the performance preferences, while the weights in [34] are just the data rates accumulated in the past. Finally, the optimal control rate τ of OMA-enabled V2X is provided. Since the τ of OMA is far less than that in NVRA, the superiority of NOMA-enabled V2X to OMA-enabled V2X can be verified.

B. IMPACTS OF DISTRIBUTION OF VEHICLES ON THE RESOURCE ALLOCATION SCHEME

To evaluate the impacts of distribution of vehicles on the resource allocation scheme, a snapshot of vehicles' positions is displayed, where we set $M = 12, K = 3, N = 4$ and identical weights are considered. In Fig. 6(a), the circle

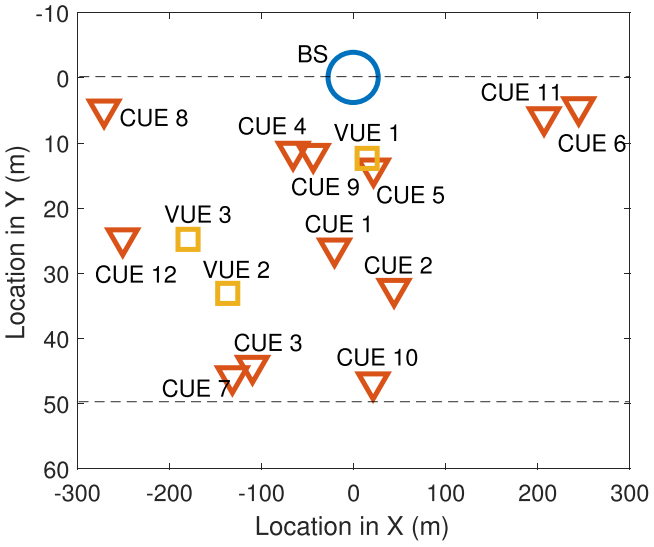

(a)

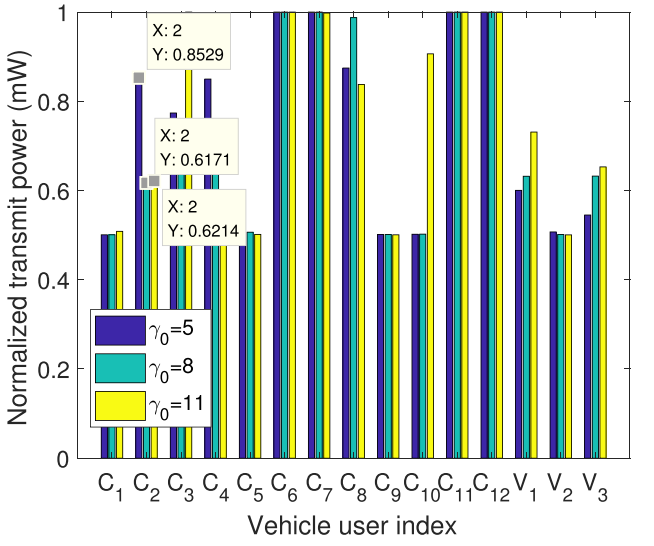

(b)

FIGURE 6. (a) A snapshot of vehicles' position. The blue circle represents the BS, and the red triangle represents the CUEs. Moreover, VUE pairs are denoted by yellow square. (b) Normalized allocated power of CUEs and VUE pairs with different γ_0. ($N = 12, K = 3, N = 4$).

located at original point denotes the BS with a cell radius of $300m$. The triangles and squares represent CUEs and VUE pairs, respectively. In addition, the highway is between the two dash lines and its width is assumed to be $50m$. To obtain a resource allocation scheme for the situation in Fig. 6(a), NVRA algorithm is applied and the corresponding results are displayed in Fig. 6(b) and Tab. 2, where the transmit power is normalized via sigmoid function and vehicle user index is denoted by C_i and V_j. From Fig. 6(b) and Tab. 2, it can be noted that the CUEs in one cluster are dispersed along the highway, which indicates that the channel gains of these CUEs may quite different. Meanwhile, Fig. 6(b) shows that the CUE nearest to the BS in one cluster is allocated

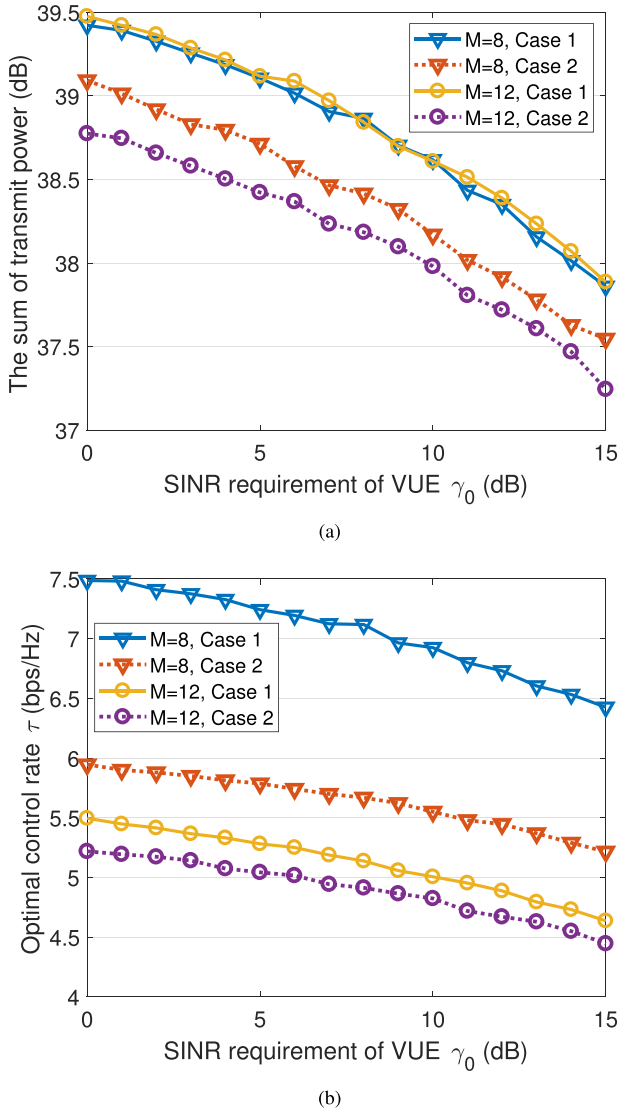

FIGURE 7. (a) The impact of γ_0 on the sum of transmit power with different M. (b) The impact of γ_0 on the optimal control rate τ with different M. ($K = 3$, $N = 4$).

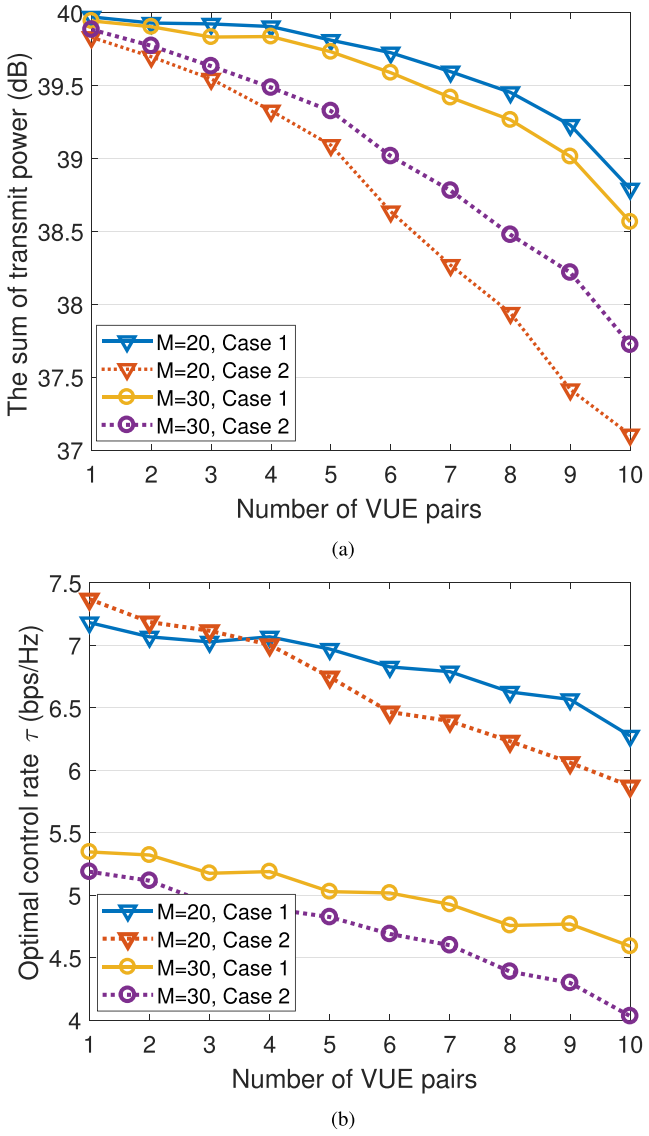

FIGURE 8. (a) The impact of K on the sum of transmit power with different M. (b) The impact of K on the optimal control rate τ with different M. ($N = 10$, $\gamma_0 = 8$dB).

the lowest transmit power and the farthest CUE is allocated the highest transmit power. Furthermore, if γ_0 is increased, the optimal control rate τ^* will decrease and the resource allocation results may change.

C. IMPACTS OF V2V LINKS ON THE RESOURCE ALLOCATION SCHEME

In Fig. 7, the impacts of γ_0 on the sum of transmit power $\sum_{i\in\mathcal{M}} p_i$ and the optimal control rate τ are illustrated, where we set $K = 3$ and $N = 4$. Both Case 1 and Case 2 are considered and the weights in Case 2 are randomly generated. In order to make the figures comparable, the sum of weights is assumed to be M. Consequently, the optimal control rate τ can be regarded as the average throughput of M CUEs. To enhance the reliability of V2V links, a higher SINR requirement of VUEs is introduced. From Fig. 7(a), it can be noticed that the sum of transmit power will decrease when γ_0 grows larger, which means that the interference to VUE pairs caused by the BS is reduced. Correspondingly, the performance of the optimal control rate τ is displayed in Fig. 7(b). It is obvious that the decreased transmit power results in a lower τ for a certain M. Moreover, in both Case 1 and Case 2, since the total transmit power of the BS is fixed, the decrease of the number of CUEs will improve the optimal control rate τ, which means that the average transmit power of CUEs is raised. Furthermore, due to the randomness of the weights in Case 2, we cannot draw the conclusion that the optimal control rate τ in Case 1 is larger than that in Case 2. As an extreme example, we assume that the weight of the CUE with the highest channel gain is much larger than the others. Thus, this CUE will occupy most of the allocated

power. Due to its high channel gain, the average τ must be higher than that in Case 1.

In Fig. 8, we evaluate the impacts of K on the sum of transmit power $\sum_{i\in\mathcal{M}} p_i$ and the optimal control rate τ. In this scenario, the number of SCs is set to be 10 and γ_0 equals to 8dB. From the figures, it can be observed that the performance of V2I links is affected by the number of V2V links due to the SC sharing. In Fig. 8(a), the sum of transmit power is reduced by around 1.5dB when K increases from 1 to 10 for both $M = 20$ and $M = 30$ in Case 1. While in Case 2, the sum of transmit power is more sensitive to the number of VUE pairs. It is easy to understand that the CUE with a higher weight in Case 2 must be allocated more power than that in Case 1. Thus, to guarantee the reliability of V2V links, the CUEs which are allocated higher transmit power are more likely subject to constraints. As a result, the sum of transmit power in Case 2 experiences a large attenuation when K grows due to the notable difference of CUEs' allocated power. In Fig. 8(b), the optimal control rate τ versus the number of VUE pairs K with different M is illustrated. As can be seen, the optimal control rate τ is about 7bps/Hz when two CUEs share one SC (i.e., $M = 20$). And when three CUEs share one SC (i.e., $M = 30$), τ is around 5bps/Hz.

V. CONCLUSIONS

In this paper, the resource allocation problem has been investigated for both CUEs and VUEs in a downlink NOMA-enabled V2X network. To satisfy the fairness and variety requirements of CUEs for data service, the weighted max-min rate fairness is considered. Meanwhile, the reliability of V2V links is guaranteed by imposing minimum SINR requirements on problem formulation. To address this issue, a low-complexity and effective NVRA algorithm is proposed, which is suitable for both identical weights and different weights. Furthermore, the convergence of NVRA algorithm can be verified by theoretical analysis and simulation results. When compared to exhaustive search method, NVRA algorithm can achieve a near optimal performance with a significantly lower computational complexity for large M, K and N. Moreover, the simulation results show that the CUEs in one cluster are probable with diverse channel gains. Since the requirements of CUEs and VUEs conflict with each other, the impact of V2V links on the resource allocation scheme is evaluated, which indicates that the optimal control rate, τ, will decrease with the increase of the number of V2V links and the minimum SINR requirements of VUE pairs.

REFERENCES

[1] Z. MacHardy, A. Khan, K. Obana, and S. Iwashina, "V2X access technologies: Regulation, research, and remaining challenges," *IEEE Commun. Surveys Tuts.*, vol. 20, no. 3, pp. 1858–1877, 3rd Quart., 2018.

[2] G. Karagiannis *et al.*, "Vehicular networking: A survey and tutorial on requirements, architectures, challenges, standards and solutions," *IEEE Commun. Surveys Tuts.*, vol. 13, no. 4, pp. 584–616, 4th Quart., 2011.

[3] *Intelligent Transport Systems (ITS); Vehicular Communications; Basic Set of Applications; Definitions*, document TR 102 638 V1.1.1, European Telecommunications Standards Institute, Sophia Antipolis, France, 2009.

[4] A. Karapantelakis and J. Markendahl, "The role of mobile network operators in intelligent transport systems: Situation analysis, challenges and suggested approach," in *Proc. Int. Telecommun. Soc. Reg. Conf. (ITS)*, Los Angeles, CA, USA, Oct. 2015, pp. 1–7.

[5] M. Shulman and R. K. Deering, "Third annual report of the crash avoidance metrics partnership, April 2003–March 2004," Nat. Highway Traffic Saf. Admin., Farmington Hills, MI, USA, Tech. Rep. DOT HS 809 663, Jan. 2005.

[6] S. Chen *et al.*, "Vehicle-to-everything (V2X) services supported by LTE-based systems and 5G," *IEEE Commun. Standards Mag.*, vol. 1, no. 2, pp. 70–76, Jun. 2017.

[7] L. Liang, G. Y. Li, and W. Xu, "Resource allocation for D2D-enabled vehicular communications," *IEEE Trans. Commun.*, vol. 65, no. 7, pp. 3186–3197, Jul. 2017.

[8] S. Chen, J. Hu, Y. Shi, and L. Zhao, "LTE-V: A TD-LTE-based V2X solution for future vehicular network," *IEEE Internet Things J.*, vol. 3, no. 6, pp. 997–1005, Dec. 2016.

[9] Q. Wei, L. Wang, Z. Feng, and Z. Ding, "Wireless resource management in LTE-U driven heterogeneous V2X communication networks," *IEEE Trans. Veh. Technol.*, vol. 67, no. 8, pp. 7508–7522, Aug. 2018.

[10] L. Liang, J. Kim, S. C. Jha, K. Sivanesan, and G. Y. Li, "Spectrum and power allocation for vehicular communications with delayed CSI feedback," *IEEE Wireless Commun. Lett.*, vol. 6, no. 4, pp. 458–461, Aug. 2017.

[11] B. W. Khoueiry and M. R. Soleymani, "An efficient NOMA V2X communication scheme in the Internet of vehicles," in *Proc. IEEE 85th Veh. Tchnol. Conf. (VTC-Spring)*, Sydney, NSW, Australia, Jun. 2017, pp. 1–7.

[12] Z. Ding, X. Lei, G. K. Karagiannidis, R. Schober, J. Yuan, and V. Bhargava, "A survey on non-orthogonal multiple access for 5G networks: Research challenges and future trends," *IEEE J. Sel. Areas Commun.*, vol. 35, no. 10, pp. 2181–2195, Oct. 2017.

[13] S. M. R. Islam, N. Avazov, O. A. Dobre, and K.-S. Kwak, "Power-domain non-orthogonal multiple access (NOMA) in 5G systems: Potentials and challenges," *IEEE Commun. Surveys Tuts.*, vol. 19, no. 2, pp. 721–742, 2nd Quart., 2017.

[14] Z. Qin, X. Yue, Y. Liu, Z. Ding, and A. Nallanathan, "User association and resource allocation in unified NOMA enabled heterogeneous ultra dense networks," *IEEE Commun. Mag.*, vol. 56, no. 6, pp. 86–92, Jun. 2018.

[15] Y. Liu, Z. Qin, M. Elkashlan, A. Nallanathan, and J. A. McCann, "Non-orthogonal multiple access in large-scale heterogeneous networks," *IEEE J. Sel. Areas Commun.*, vol. 35, no. 12, pp. 2667–2680, Dec. 2017.

[16] Q. Wei, W. Sun, B. Bai, L. Wang, E. G. Ström, and M. Song, "Resource allocation for V2X communications: A local search based 3D matching approach," in *Proc. IEEE Int. Conf. Commun. (ICC)*, Paris, France, May 2017, pp. 1–6.

[17] W. Sun, D. Yuan, E. Ström, and F. Brännström, "Cluster-based radio resource management for D2D-supported safety-critical V2X communications," *IEEE Trans. Wireless Commun.*, vol. 15, no. 4, pp. 2756–2769, Apr. 2016.

[18] C.-Y. Wei, A. C.-S. Huang, C.-Y. Chen, and J.-Y. Chen, "QoS-aware hybrid scheduling for geographical zone-based resource allocation in cellular vehicle-to-vehicle communications," *IEEE Commun. Lett.*, vol. 22, no. 3, pp. 610–613, Mar. 2018.

[19] W. Huang, L. Ding, D. Meng, J.-N. Hwang, Y. Xu, and W. Zhang, "QoE-based resource allocation for heterogeneous multi-radio communication in software-defined vehicle networks," *IEEE Access*, vol. 6, pp. 3387–3399, 2018.

[20] Y. Liu, Z. Qin, M. Elkashlan, Z. Ding, A. Nallanathan, and L. Hanzo, "Nonorthogonal multiple access for 5G and beyond," *Proc. IEEE*, vol. 105, no. 12, pp. 2347–2381, Dec. 2017.

[21] Y. Cai, Z. Qin, F. Cui, G. Y. Li, and J. A. McCann, "Modulation and multiple access for 5G networks," *IEEE Commun. Surveys Tuts.*, vol. 20, no. 1, pp. 629–646, 1st Quart., 2018.

[22] J. Zhao, Y. Liu, K. K. Chai, Y. Chen, and M. Elkashlan, "Joint subchannel and power allocation for NOMA enhanced D2D communications," *IEEE Trans. Commun.*, vol. 65, no. 11, pp. 5081–5094, Nov. 2017.

[23] L. Lei, D. Yuan, C. K. Ho, and S. Sun, "Power and channel allocation for non-orthogonal multiple access in 5G systems: Tractability and computation," *IEEE Trans. Wireless Commun.*, vol. 15, no. 12, pp. 8580–8594, Dec. 2016.

[24] Y. Liu, M. Elkashlan, Z. Ding, and G. K. Karagiannidis, "Fairness of user clustering in MIMO non-orthogonal multiple access systems," *IEEE Commun. Lett.*, vol. 20, no. 7, pp. 1465–1468, Jul. 2016.

[25] L. P. Qian, Y. Wu, H. Zhou, and X. Shen, "Non-orthogonal multiple access vehicular small cell networks: Architecture and solution," *IEEE Netw.*, vol. 31, no. 4, pp. 15–21, Jul./Aug. 2017.
[26] L. P. Qian, Y. Wu, H. Zhou, and X. Shen, "Dynamic cell association for non-orthogonal multiple-access V2S networks," *IEEE J. Sel. Areas Commun.*, vol. 35, no. 10, pp. 2342–2356, Oct. 2017.
[27] B. Di, L. Song, Y. Li, and G. Y. Li, "Non-orthogonal multiple access for high-reliable and low-latency V2X communications in 5G systems," *IEEE J. Sel. Areas Commun.*, vol. 35, no. 10, pp. 2383–2397, Oct. 2017.
[28] B. Di, L. Song, Y. Li, and Z. Han, "V2X meets NOMA: Non-orthogonal multiple access for 5G-enabled vehicular networks," *IEEE Wireless Commun.*, vol. 24, no. 6, pp. 14–21, Dec. 2017.
[29] M. S. Ali, H. Tabassum, and E. Hossain, "Dynamic user clustering and power allocation for uplink and downlink non-orthogonal multiple access (NOMA) systems," *IEEE Access*, vol. 4, pp. 6325–6343, Aug. 2016.
[30] L. Zheng, D. W. H. Cai, and C. W. Tan, "Max-min fairness rate control in wireless networks: Optimality and algorithms by Perron-Frobenius theory," *IEEE Trans. Mobile Comput.*, vol. 17, no. 1, pp. 127–140, Jan. 2018.
[31] B. Yaw and H. W. Kuhn, "The Hungarian method for the assignment problem," *Naval Res. Logistics Quart.*, vol. 2, pp. 83–97, Mar. 1955.
[32] J. Zhao, Y. Liu, K. K. Chai, M. Elkashlan, and Y. Chen, "Matching with peer effects for context-aware resource allocation in D2D communications," *IEEE Commun. Lett.*, vol. 21, no. 4, pp. 837–840, Apr. 2017.
[33] J. Zhao, Y. Liu, K. K. Chai, Y. Chen, and M. Elkashlan, "Many-to-many matching with externalities for device-to-device communications," *IEEE Wireless Commun. Lett.*, vol. 6, no. 1, pp. 138–141, Feb. 2017.
[34] J. Choi, "Power allocation for max-sum rate and max-min rate proportional fairness in NOMA," *IEEE Commun. Lett.*, vol. 20, no. 10, pp. 2055–2058, Oct. 2016.

HANYU ZHENG received the B.Sc. degree in information engineering from the Beijing Institute of Technology, Beijing, China, in 2013, where he is currently pursuing the Ph.D. degree with the School of Information and Electronics. His research interests include radio resource management, non-orthogonal multiple access, and V2X communications.

HAI LI (M'05) received the B.Sc. and Ph.D. degrees from the Beijing Institute of Technology, Beijing, China, in 1997 and 2002, respectively. He is currently an Associate Professor with the School of Information and Electronics, Beijing Institute of Technology. His research interests include signal processing, protocol engineering, and wireless communications.

SHUJUAN HOU received the B.Sc., M.Sc., and Ph.D. degrees from the Beijing Institute of Technology, Beijing, China, all in signal and information processing. She is currently an Associate Professor with the School of Information and Electronics, Beijing Institute of Technology. Her main research interests are digital signal processing and radio resource management in wireless communications.

ZHENGYU SONG received the B.Sc. and M.Sc. degrees from Beijing Jiaotong University, Beijing, China, and the Ph.D. degree from the Beijing Institute of Technology, Beijing, all in information and communication engineering. He is currently with the School of Electronic and Information Engineering, Beijing Jiaotong University. His main research interests include radio resource management in multicarrier systems, non-orthogonal multiple access, heterogeneous networks, and mobile edge computing.